1   **Application of a handheld X-ray fluorescence spectrometer**

2   **for real-time, high-density quantitative analysis of drilled**

3   **igneous rocks and sediments during IODP Expedition 352**

4

5   **J.G. Ryan[1], J.W. Shervais[2], Y. Li[3], M.K. Reagan[4], H.Y. Li[5], D. Heaton[6], M.**

6   **Godard[7], M. Kirchenbaur[8], S. Whattam[9], J.A. Pearce[10], T. Chapman[11], W.**

7   **Nelson[12], J. Prytulak[13], K. Shimizu[14], K. Petronotis[15], and the IODP Expedition**

8   **352 Scientific Team[16]**

9   [1]{School of Geosciences, University of South Florida, Tampa, FL, USA}
10 [2]{Geology, Utah State University, USA}
11 [3]{Institute of Geology, Chinese Academy of Geological Sciences, Beijing, China}
12 [4]{Dept. Earth and Environmental Sciences, University of Iowa, Iowa City, USA}
13 [5]{State Key Laboratory of Isotope Geochemistry, Guangzhou Institute of Geochemistry,
14 Chinese Academy Science, Guangzhou 510640, China}
15 [6]{College of Earth, Ocean and Atmospheric Sciences, Oregon State Univ., Corvallis, OR}
16 [7]{Geosciences, Universite Montpellier II, Montpellier, France}
17 [8]{Geologische Inst., Universitat Koln, Koln, Germany}
18 [9]{Dept. Earth and Environmental Sciences, Korea University, Republic of Korea}
19 [10]{Earth and Ocean Sciences, Cardiff University, UK}
20 [11]{School of Geosciences, University of Sydney, Australia}
21 [12]{Physics, Astronomy, Geosciences; Towson University, MD, USA}
22 [13]{Earth Sciences and Engineering, Imperial College, UK}
23 [14]{International Ocean Discovery Program, College Station, TX, USA}
24 [15] {Kochi Core Center, Kochi University, Japan}
25 [16]{R. Almeev, A. Avery, C. Carvallo, G. Christeson, E. Ferre, W. Kurz, S. Kutterolf, K.
26 Michibayashi, S. Morgan, M. Python A. Robertson, W. Sager, T. Sakuyama; see
27 http://iodp.tamu.edu/scienceops/precruise/izuboninforearc/participants.html for affiliations}
28
29 Correspondence to: J. G. Ryan (ryan@mail.usf.edu)
30

31 **Abstract**

32   Handheld energy dispersive portable X-ray spectrometers (pXRF) are generally designed

33 and used for qualitative survey applications. We developed shipboard quantitative analysis

34 protocols for pXRF and employed the instrument to make over 2000 individual abundance

35 measurements for a selection of major and trace elements on over 1200 meters of recovered

36 core during the eight weeks of the International Ocean Discovery Program (IODP) Expedition

37 352 to the Izu-Bonin forearc. pXRF analytical performance, accuracy and precision were

38 found to be the same on powdered rock samples and on freshly cut rock surfaces, and sample

1 results were similar within error to measurements made via shipboard ICP-OES analysis save

2 at low abundance levels for a few elements. Instrument performance was optimal for

3 elements between Z=19 and Z=40, and the system yielded reproducible data for K, Ca, Ti, V,

4 Cr, Mn, Fe, Cu, Zn, Rb, Sr, and Zr on both powdered samples and rock surfaces. Working

5 curves developed via pXRF measurement of a suite of geologic standard reference materials

6 and well-characterized lavas permitted accurate quantitative measurements for many of the

7 examined elements on both sample powders and rock surfaces. Although pXRF has been

8 sporadically employed on previous cruises, Expedition 352 is the first time a detailed, high-

9 density chemostratigraphy of recovered core samples was collected using pXRF

10 measurements of rock core surfaces. These high-resolution data allowed the recognition of

11 chemically distinct eruptive units in near real-time. The rapid identification of geochemical

12 trends vastly improved our selection of samples for shipboard and shore-based analysis,

13 permitted a more comprehensive interpretation of our Expedition results, and provided key

14 decision-making information for drilling operations.

15

16

17 **1   Introduction**

18   A significant challenge faced in oceanic drilling expeditions is the ability to perform

19 basic chemical characterization of recovered materials in a timely enough fashion to monitor

20 rock type and downhole stratigraphic information during coring. While it is established

21 practice to cut thin sections and conduct bulk chemical analysis of recovered samples as they

22 are collected, these procedures typically require several days to complete. This can pose

23 significant challenges during hard-rock drilling, because recovery in igneous rocks is often

24 poor, and volcanic igneous rocks in particular may not exhibit clear mineralogical, textural, or

25 other macroscopic characteristics that permit ready classification.

26   International Ocean Discovery Program (IODP) Expedition 352 aimed to drill a complete

27 volcanic reference section in the Izu-Bonin outer forearc (Reagan et al., 2015). Over 1200 m

28 of basaltic and boninitic lavas were drilled, with limited to poor recovery (~12% in basalts;

29 ~30% in boninites; see Reagan, et al 2015). While variations in eruptive style and alteration

30 were at times evident, some recovered samples were phenocryst-poor and uniform in

31 appearance. Thin sectioning of samples and ICP-OES measurements on the *JOIDES*

32 *Resolution* (*JR*) permitted the characterization of recovered samples for phenocryst

33 assemblages as well as major oxides and selected high-abundance trace elements. However,

poor correlation between phenocryst and compositional variations, the substantial time lag between sample recovery and geochemical analysis (~1 week to powder, digest, and analyze samples via ICP-OES), and limits on the number of samples that could feasibly be processed and analyzed on the ship severely impact the ability to track volcanic rock compositions downhole in real time. Such knowledge of downhole variation is often crucial for operational decision-making.

Seeking a better means for rapid and quantitative chemical characterization of drill core, the Expedition 352 geochemistry and petrology scientists turned to a handheld portable X-ray fluorescence spectrometer (pXRF), which was available onboard for the expedition, but had not been previously employed for real time hard-rock core characterization. pXRF has been used widely to identify contaminants in soils, to assay the provenance of geo-archaeological materials, and to characterize cultural materials in archaeology (see Potts and West 2008; Zhu et al 2011; Weindorf et al 2012; Conrey et al 2014; Hu et al 2014; Swanhart et al 2014; Tykot, 2016, among others). The uses of pXRF and related methods such as X-ray core scanning in marine geological applications have mostly focused upon the characterization of recovered submarine sediments (e.g., Wien et al 2005; Kido et al 2006; Jan Weltje and Tjallinge, 2008; Lowemark et al 2011; Hennekam and deLange, 2012; Liang et al 2012; Rowe et al 2012). Aside from offering quick measurements (1-2 minutes for fresh sample surfaces and/or powders), we found that the method provided quantitative results at reasonable precision and accuracy for a selection of useful major and trace elements, which permitted the rapid characterization of recovered core samples, as well as straightforward correlations with and confirmations of ICP-OES sample powder results.

2 Methods

2.1 Instrumentation

The shipboard pXRF available on the *JOIDES Resolution* was a Fisher Niton GOLDD+ XL3t handheld instrument, and included sample holders for both round mounts and larger rock pieces (Figure 1).   An additional shielded mounting system had been constructed by IODP for pXRF use on larger sections of core.   The instrument had been tested to a very limited degree on previous Expeditions (330, 335, 345, 350; see "XRF" in Teagle et al, 2012; also Koppers et al 2012; Gillis et al 2014). The Niton GOLDD+ XL3t is a self-contained energy-dispersive XRF survey instrument with a variable intensity X-ray source (6-50 kV, 0-200 μA Ag anode) and a proprietary GOLDD (Geometrically Optimized Large Area Drift

1 Detector) detection system that is rated by the manufacturer for low detection limit, high-

2 precision measurement of 30+ elements, though a helium purge is required to obtain results

3 on lower atomic number species (Thermo Scientific, 2016). The instrument includes data

4 correction packages tailored to a variety of applications (metals, plastics, soils and minerals,

5 and consumer goods), and reads out concentration results for each measurement, simplifying

6 data reduction and interpretation. In terms of the specifics of the X-ray technology, the Niton

7 GOLDD+ XL3t instrument differs markedly from wavelength-dispersive XRF instruments

8 that had been used on the *JOIDES Resolution* in the past (see Christie et al, 2001 as an

9 example), especially in that extensive sample preparation is not required. The X-ray analysis

10 strategies of this instrument are more sophisticated than either the tabletop EDS-XRF system

11 employed at sea by Wien et al (2005), or than X-ray core scanners (e.g., Jan Weltje and

12 Tjallinge, 2008; Lowemark et al 2011). It is more directly comparable to the handheld

13 portable XRF instruments described by Weindorf et al (2012) and Rowe et al (2012), albeit

14 with a newer generation detection system and data correction and processing protocols. On

15 Expedition 352, we utilized its "Soils" protocol within the "Soils and Minerals" submenu, as

16 this protocol, which permits calibration on a large number of elements, provided the most

17 reliable concentration results. The Soils protocol is designed to make measurements per US

18 EPA Method 6200 (Thermo Fisher, 2010; USEPA, 2007). The instrument utilizes several

19 excitation filters that optimize instrument sensitivity for measuring elements in four different

20 X-ray energy ranges: the "light" range (for low atomic number elements such as Si, Al and

21 Mg); the "Low" range (which optimizes for Cr, V, Ti, Sc, Ca, K, and S); the "Main" range

22 (optimized for Mo, Zr, Sr, U, Rb, Th, Pb, Au, Se, As, Hg, Zn, W, Cu, Ni, Co, Fe, and Mn);

23 and the "High" range (optimized for Ba, Cs, Te, Sb, Sn, Cd, Ag, and Pd). The Soils protocol

24 applies a modified Compton normalization method for calibration, (i.e., calibration is based

25 on the measurement of a single specific reference sample, recommended in the user manual as

26 the CCRMP TILL-4: Thermo Fisher, 2010; CCRMP, 1995: Table 1). This initial calibration

27 was completed at the factory before the Expedition. "Light" range species can only be

28 measured with a helium purge, which was not available on the ship. Elements in the "High"

29 energy range did not provide reliable results, as most were below their practical detection

30 limits in our samples.   "Main" and "Low" energy range species, however, yielded results that

31 were sufficiently precise and accurate for a number of elements when concentrations were

32 above instrument detection limits.

2.2   *Elements Detected, Correlation and Accuracy*

The elements found to be reliably above instrument detection limits in Expedition 352 materials were Fe, Ca, Mn, Ti, K, Sr, Zr, Cu, Zn, V, and Cr. Ni was above detection limits in our highest-concentration reference materials, like ultramafic rock samples (e.g., USGS Reference material DTS-1 or Geological Survey of Japan reference material JP-1), as well as in some of the boninitic igneous rocks examined during Expedition 352. However it was too close to the pXRF detection limit in many of the other standard reference materials available onboard to develop reasonable working curves (Ni reported level of detection = 25 ppm: Teagle et al 2012; Table 2). Scandium was consistently above detection limits, but yielded scattered and un-correlated results that were 3–10 times actual abundances based on reference materials. Thus, Sc and Ni were therefore not measured by pXRF during Expedition 352.

Correlation curves developed for Fe, Ca, Mn, Ti, K, Sr, Zr, Cu, Zn, V, and Cr (i.e., plots of pXRF abundances as per the soils correction protocol versus reported consensus values for reference materials: Table 3; Figure 2) were of varying quality, but many yielded correlation coefficients (*r* values) of 0.95 or better, indicating high consistency in instrument performance over a range of concentrations. *Y*-intercept values were significantly offset from the origin for several of the higher abundance elements (Figure 2), in particular Fe. It is probable that this is an effect of the Compton normalization strategy, as Compton normalization can be problematic for elements that show a wide range in abundances, and/or are substantially higher than the values of the standard used (Thermo Fisher 2010), though it may also reflect differences sample matrices (i.e., basaltic/boninitic and ultramafic rocks rich in Fe, Ca, and Mg, vs. glacial till (Table 1)). In addition, the Compton scattered tube line is less effective at estimating mass absorption below the Fe absorption edge, which leads to non-linear response (Reynolds 1963). In the case of iron, the resultant working curve had a high r value, with a negative *y* intercept of >2% wt; for Ca, the *y* intercept of the working curve was also negative, but consistently within <0.5% wt. of the origin, so this effect appeared to be less of a concern. Our correlation curve for vanadium had a low r value (due at least in part to low-precision V concentration data for some of the reference materials available on the ship), but pXRF results for V were found to be highly reproducible and at expected abundance levels for the samples examined during Expedition 352, suggesting that for V the pXRF was at least producing an internally consistent data set.

In general, decisions to accept pXRF results for a particular element were based on the correlation curve quality of fit (*r* values of 0.95 or better), slopes approximating 1.0 (0.9–1.1),

1 and *y*-intercepts approaching the origin within analytical uncertainties. Data for elements with

2 correlation curves showing substantial offsets in their *y*-intercepts and for elements with

3 correlation curve *r* values of <0.95 were generally not utilized in our interpretations. For the

4 remaining elements, the correlation curves in Figure 2 became the basis for working curves to

5 calculate accurate elemental concentrations. These curves were reliable over the concentration

6 ranges constrained by our reference materials.

7

2.43 Calibration and use on sample powders and rock surfaces

9   Working curves for the different elements measured by pXRF were produced using

10 powder mounts of international reference standards (BHVO-2; BCR-2, JB-2, JB-3, AGV-1,

11 MRG-1, JP-1, and DTS-1: Table 1). Additionally, we made use of several previously

12 analyzed Chichijima Island boninite samples (J. Pearce, pers. comm., 2014; Table 1) to

13 provide additional calibration data for boninites, which have unusual compositional profiles.

14 The standards correlation data were evaluated with Microsoft Excel using the LINEST

15 function to produce slope and intercept values (see Figure 2 for the shipboard working curve

16 calculations) that were used to correct the readout concentration data from the instrument

17 relative to accepted standard values, and a correction algorithm was developed for each

18 analyzed element as part of a single data correction spreadsheet. Newly collected pXRF data

19 from rock cores or powders on the ship were all corrected via this approach before their final

20 tabulation and use in the geochemical analysis of recovered materials.

21   Powdered samples were prepared for analysis using re-usable plastic powder mount

22 assemblies. These sample mounts were designed to fit in the sample holder system provided

23 with the instrument (Figure 1), and yielded consistent results on repeated analysis (i.e., Table

24 3). Mounts of our pXRF calibration standards were maintained and periodically re-measured

25 during the Expedition, while mounts of powdered unknowns were prepared, measured and

26 disassembled, with the mounts recycled for use as needed.

27

2.4   Measurement protocols and performance tests on Expedition 352
recovered materials

30   pXRF measurements on unknowns (sample powders or rock surfaces) were 60 seconds

31 each on the Low, Main, and High range filter elements. Longer count times were possible,

32 and as with any X-ray analysis system longer counting times served to improve overall

1 precision. However, given that our results were sufficiently reproducible at 60 seconds we

2 chose not to measure for longer periods. Typically three measurements across all three ranges

3 were averaged as a single determination on powdered samples. For rock surfaces three or

4 more measurements at several different positions on the sample constituted a single analysis.

5   The long-term reproducibility of the pXRF instrument was tracked through a month of its

6 use on the ship through repeated analyses of the USGS reference material BHVO-2 (Table 3).

7 Variability in pXRF results over time was within the instrument's reported measurement

8 uncertainties for all the elements analyzed (Table 3), with no evidence for signal drift over the

9 course of our usage. The accuracy of data for Fe and V were poor, for reasons noted above;

10 issues with the accuracy of Cr data at the abundance levels for BHVO-2 are discussed below.

11   To assay the performance of the shipboard pXRF instrument on the different kinds of

12 sample materials we encountered on Expedition 352, we conducted tests comparing results on

13 rocks versus powdered samples, and on rock surfaces.

14   To test the pXRF performance on rock samples as compared to sample powders, we

15 measured with the pXRF a selection of basaltic sample powders from Hole U1440B that had

16 been prepared for ICP-OES analysis and compared these data to measurements on the fresh

17 cut surfaces of thin section billets taken adjacent to each sampling site. The powdered

18 samples were intentionally selected from large, homogeneous core sections, and these became

19 "POOL" samples on which all shipboard scientists would collect data (e.g., Reagan et al

20 2015). A thin section billet was taken from the same cut core segment for each of the

21 "POOL" samples to provide petrographic context. Comparisons between pXRF analyses on

22 these powders and thin section billets are illustrated in Figure 3.

23   Possible outcomes for this kind of comparison would be broad abundance similarities

24 between the powders and billets, or potentially significant variability resulting from

25 mineralogical variations in the rock samples and/or differences in packing density of particles

26 in powdered samples with respect to solid rock. Another important concern regarding data

27 quality would be any evidence of systematic differences in abundance levels for all or some

28 elements that might indicate differences in the pXRF response on powders versus rocks. We

29 found good correlations between pXRF data for un-oxidized "POOL" sample powders and the

30 corresponding thin section billets from Hole U1440B for those elements that were not

31 strongly affected by secondary alteration processes, with variability that was at or within the

32 measurement uncertainties of the elements examined (Figure 3). The elements analyzed that

33 were more sensitive to alteration effects (K, Sr, and to a lesser extent Ca) show greater

1 variability, though even in the case of K, which shows the greatest scatter, most samples are

2 within error of a 1:1 relationship. For these elements, inhomogeneous distribution in

3 secondary minerals may be producing some local variability, but this effect is not evident for

4 the more immobile elements we measured. There was no obvious evidence for performance

5 differences related to material preparation. The pXRF appears to provide comparable results

6 for the selected elements on both powdered and solid-rock versions of what was

7 approximately the same sample material. Thus, for the relatively uniform, aphanitic volcanic

8 rocks encountered in Hole U1440B and at the other Expedition 352 drilling locations, direct

9 pXRF measurements of rock surfaces yielded data that could be directly compared to data

10 derived from powdered samples.

11   A significant concern with the quantitative analytical use of the pXRF is the degree to

12 which within-sample compositional variability might complicate the interpretation of

13 measured results. To evaluate this issue, a thin section billet from a previously analyzed

14 basaltic rock sample from our field area (Sample 1090-20; Reagan et al., 2010), comparable

15 compositionally and texturally to Site U1440B recovered basalts, was analyzed multiple times

16 at a variety of different positions on the sample's cut surface. The results of this test are

17 presented in Table 4. The standard deviation of our analyses varied by element as a function

18 of overall abundance level and instrument performance, with some elements showing as little

19 as 3% overall variation. The resulting analyses were largely comparable to the published

20 results for this sample (e.g., Reagan et al 2010), as constrained by the calibration of the

21 instrument and our approach (see Figure 2 and discussion below), indicating that for the fine

22 grained igneous rocks recovered at Site U1440 and similar igneous rock samples from the

23 other Expedition 352 sites, within-sample variability is not a significant concern.

24

25 ***2.5: Comparisons of pXRF performance to other analytical methods***

26   On the ship we made comparisons of our pXRF results with measurements made using

27 the shipboard ICP-OES (Reagan et al 2015). While ICP-OES measurements were conducted

28 on solutions made via lithium borate fusions of sample powder aliquots, which had been

29 heated in a muffle furnace for Loss on Ignition determinations, pXRF measurements were

30 made directly on these oxidized powders. Subsequently, all of the "POOL" sample powders

31 from Expedition 352 have been analyzed onshore via wavelength-dispersive XRF methods

32 (Godard et al 2015; Shervais et al 2016), permitting a more comprehensive evaluation of the

33 different methods. Our shore based wavelength dispersive XRF measurements were made on

1 fused beads with 1:5 ratio of sample to Li-borate flux, and analyzed with a Panalytical 2400

2 XRF. Figure 4 presents pXRF:ICP-OES:XRF comparison plots for key elements in our

3 "POOL" sample suite.

4   In Figure 4, it is evident that for all of these elements, there are systematic correlations

5 within error between our pXRF results and results obtained on the ship via ICP-OES, and

6 onshore via wavelength dispersive XRF. The correlations for each element vary in terms of

7 slope and intercept, with some elements (Ti, K) showing intercepts very near zero, and slopes

8 approaching 1.0. The Ca correlations versus the ICP-OES and XRF show slopes near 1.0, but

9 the pXRF data are shifted to lower values, resulting in a non-zero intercept. These

10 correlations are consistent with what was observed in the pXRF Ca correlation curve for

11 standards in Figure 2. The pXRF Ti data shows scatter not evident in the other methods,

12 which most likely relates to direct measurement of oxidized powders with pXRF, whereas the

13 other two methods measured fusion beads, either in solution or in situ. We speculate that

14 titanomagnetite grains were inhomogeneously distributed in some of the powders analyzed by

15 pXRF.

16   For lower abundance elements, there are greater divergences in slopes among the

17 pXRF:ICP-OES and pXRF:XRF correlations (Figure 4). Sr shows excellent agreement

18 between the pXRF and XRF data with a slope near 1.0 and a near-zero intercept, while the

19 shipboard ICP-OES results show greater scatter, albeit with considerable overlap. For Cr the

20 pXRF:XRF and ICP-OES:XRF correlations are distinct, with the ICP-OES results showing

21 lower Cr contents than pXRF below 300 ppm Cr, but higher concentrations than pXRF above

22 this range, while the onshore XRF results were consistently higher. For Zr, the two

23 correlations are overlapping, with the pXRF providing consistently lower values than either

24 the ICP-OES or wavelength dispersive XRF, though given the relatively low concentrations

25 in most of our samples the actual variation is rather modest.

26   The differences in determined concentrations between the pXRF, ICP-OES, and shore-

27 based XRF systems are likely a function of calibration strategies and standard selection. In

28 the case of the Niton pXRF, we imposed an external shipboard calibration based on a range of

29 international reference samples on an existing factory-recommended Compton normalization

30 calibration scheme for the SOILS protocol, that used the CCRMP TILL-4 glacial sediment

31 reference material (Thermo Fisher 2010; CCRMP, 1995; Jochum et al 2005). Compton

32 normalization schemes only work over limited ranges in concentrations, and are best for

33 elements heavier than Ni, which may explain the problematic standards correlations for Fe

1   and Ca in Figure 2, as both run to higher values in our reference samples and recovered rocks

2   than the TILL-4 standard. Our decision to generate correlation curves using a mixture of

3   reference material types (basalts andesites, gabbros, boninites, and ultramafic rocks), while

4   necessary to cover the concentration ranges in our recovered samples, may also have

5   contributed to the variation in slope and intercept we observe in our Figure 4 correlations, as

6   strongly different sample matrices can cause non-linear signal response on all of these

7   instruments. With the shipboard ICP-OES, to minimize this problem we chose subsets of the

8   reference samples in Table 2 for calibrating different sample runs, based on the unknowns we

9   were analyzing (e.g., basaltic and gabbroic references samples for forearc basalts; boninite,

10   andesite and ultramafic reference samples for boninites); but given our usage of the pXRF

11   (see below) this kind of "tailoring" of our calibrations was not feasible.

12   Irrespective of the origins of the slope and intercept variations observed in Figure 4, the

13   shipboard Niton pXRF produces data that *correlates systematically* with results from two

14   well-established, but rather different quantitative elemental analysis methodologies. This

15   demonstrates that:

16   a) The instrument can produce data for a selection of elements that, with suitable

17   calibration, is both sufficiently precise and accurate, and

18   b) The data we collected under our described shipboard conditions can be easily

19   corrected for direct comparisons to results by other methods.

20   Because the pXRF results correlate linearly with the results from other methods (ICP-

21   OES, wavelength-dispersive XRF), these data can be used to construct a valid shipboard core

22   chemostratigraphy in real time, while core recovery and/or logging are in progress.

23   Furthermore, when widely separated core pieces are found to differ chemically, the pXRF

24   makes it possible to rapidly analyze additional pieces in order to precisely define the location

25   of chemostratigraphic boundaries.

26

27   **3   Results and Discussion**

28   The primary use of the pXRF during Expedition 352 was to conduct rapid geochemical

29   measurements of volcanic rocks encountered in the recovered cores, both through direct

30   measurements of cut rock surfaces on the archive-half core sections, and through the analysis

31   of residual thin section billets for rock samples chosen for microscopic analysis. For these

32   measurements, the sample holder system provided with the instrument was used to position

33   smaller samples, and the shielded mounting system was used for longer core segments and

1 larger rock samples (Figure 1). A built-in digital video camera in the head of the instrument

2 showed the 8 mm spot on the material that was to be analyzed, so positioning could be

3 adjusted to avoid veins and/or clearly altered zones on rock surfaces.

4   Data for all calibrated elements were collected for all samples measured via pXRF.

5 These data in some cases reproduced results for elements for which the ICP-OES afforded

6 effective measurement (Ca, K_2O, TiO_2, Cr, Zr, Sr) and for some of these species (in particular

7 TiO_2, K_2O and Sr) it offered an independent check on the accuracy of our shipboard ICP-OES

8 results. Rubidium, zinc and copper, though included in the shipboard ICP-OES analytical

9 protocols, were generally too low in concentration for successful measurement, so our pXRF

10 data for these elements effectively augmented our shipboard elemental analysis capabilities.

11 The comparable precision and accuracy of the pXRF data for powders and rock surface

12 samples, and the consistency of its results with respect to other methods, meant that the

13 extensive Expedition 352 pXRF rock surface database, collected for the purposes of

14 chemostratigraphic correlation in our cores (see below), can be integrated with our shipboard

15 ICP-OES results to provide a comprehensive geochemical profile of our recovered samples.

16   Ultimately, we used only a limited number of the elements measured via pXRF for

17 routine unit definition and stratigraphic correlation within Expedition 352 drill cores, as

18 necessitated by the constraints on time and resources aboard ship. As such, ours was a similar

19 but more targeted approach to the collection and quantitative use of pXRF data than that

20 described in Rowe et al (2012) and in other land-based studies. As key major elements

21 (specifically, Mg and Si) were not analytically accessible via the pXRF at sea, we took the

22 approach of using elemental proxies (e.g., Hastie et al 2007): abundances of the compatible

23 element Cr were used to proxy MgO abundances; Ti abundances and Ti/Zr ratios were used to

24 proxy SiO_2 as well as overall sample chemical depletion, and V abundances and V/Ti ratios

25 were used to assay source and melt oxidation state, as a possible indicator of degree of prior

26 melting of mantle sources for magmas (see Reagan et al, 2015). Strontium abundances were

27 found to be comparatively unaffected by secondary alteration processes, and were thus useful

28 in identifying the effects of plagioclase crystallization, and distinguishing between the weakly

29 subduction affected fore-arc basalts and the strongly subduction modified boninites. Data for

30 CaO and K_2O, both of which can be modified by secondary fluid-rock alteration processes,

31 were useful in assaying the freshness of samples that were prepared for ICP-OES

32 measurement on the ship, and in rectifying problems with shipboard ICP-OES measurements

33 of recovered sediments, where the inability to completely decarbonate samples during Loss

1   on Ignition procedures led to problematic major element abundance totals.   Ultimately, over

2   2000 individual pXRF analyses were made on rock surfaces and sample powders during

3   Expedition 352.

4   Using the elemental proxies approach, the shipboard Petrology team developed a detailed

5   chemostratigraphy for the recovered basalts from Sites U1440B and U1441A, and for the

6   boninitic rocks recovered at Sites U1439C and U1442A (Reagan et al, 2015; Figures 5 and 6).

7   In particular for the forearc basalts recovered from Hole U1440B, this chemostratigraphic

8   record was essential to determining unit boundaries and constraining the volcanic stratigraphy

9   of the core, as low recovery (~12%) during drilling and the highly uniform, aphyric nature of

10   the recovered basalts provided few other means for resolving among eruptive units or tracking

11   downhole changes (Figure 5).

12   In the boninite Holes U1439C and U1442A, relationships between the downhole

13   chemostratigraphy and physical properties – specifically, magnetic susceptibility – became

14   important in defining units, and in correlating what were ostensibly very different-looking

15   downhole stratigraphies for two relatively closely located sites (<1 km apart; Figure 6). In

16   both U1439C and U1442A, the detailed downhole geochemical record compiled via pXRF

17   documented clear, progressive up-section declines in TiO_2 abundances, and increases in Cr

18   abundances, pointing to a progressive depletion of the boninitic source mantle over time.

19   These progressive changes in trace element abundances are associated with a transition from

20   generally lower SiO_2 and more variably evolved boninite compositions toward the bottom of

21   each section to higher SiO_2, more magnesian boninite compositions at the top of each section.

22   These transitions are perhaps consistent with the early presence of some kind of persistent

23   magma chamber in which differentiation of boninite parental magmas could occur, followed

24   by eruptions of the more depleted, magnesian, and ostensibly primitive boninite lavas

25   observed at the tops of both sequences.

26   The real-time, high-density geochemical results provided by the pXRF informed

27   shipboard decisions on core segments to be prepared for shipboard ICP-OES analysis, and on

28   the selection of the ~100 "POOL" samples that would be the focus of coordinated shore-based

29   investigations. In addition, the pXRF data allowed the shipboard scientists to define

30   boundaries between chemostratigraphic units precisely between adjacent core pieces, and

31   guided selection of subsequent personal samples that will be used post-cruise to augment the

32   POOL sample data.

1   The advantages of our pXRF capabilities were particularly evident toward the end of

2 Expedition, when the ICP-OES ceased to be a viable analytical option due to its long lead-

3 time for completing measurements, as well as during periods of high heave and/or transits,

4 when ship movement precluded ICP operation. Our extensive pXRF dataset facilitated a more

5 intensive and sophisticated at-sea analysis and interpretation of our recovered samples (e.g.,

6 Reagan et al 2015) than would have otherwise been possible. These data also proved crucial

7 in the cost-benefit analyses of whether to continue or terminate drilling at a particular hole

8 when difficulties were encountered.

9   The flexibility of the pXRF instrumentation and approach also permitted the quantitative

10 re-examination of archived drill cores. During Exp. 352, we re-analyzed and directly

11 compared the pXRF compositions of rock surfaces from the archive halves of cores from

12 Deep Sea Drilling Program (DSDP) Leg 60 (Mariana forearc) to those of samples from our

13 Expedition, confirming their geochemical kinship and clarifying the chemical differences

14 between samples from these two different localities. Limitations on pXRF capabilities

15 associated with cores containing significant pore water, as had been reported on in past efforts

16 with shipboard X-ray core scanning instruments (i.e., Kido et al 2006; Weltje and Tjallingi

17 2008; Hennekem and de Lange 2012) were not an issue with the samples recovered on

18 Expedition 352. The fine-grained and uniform nature of many of our recovered samples made

19 Expedition 352 a nearly ideal testbed for this analytical tool and approach, though the robust

20 and flexible nature of the instrumentation suggests that even with less ideal sample types (i.e.,

21 coaser grained gabbroic/granitic rocks) useful results could be obtained with proper

22 precautions.

23

24 **4 Conclusions**

25   Modern energy-dispersive portable XRF analyzers permit the reproducible quantitative

26 determination of a menu of major and trace elements from Z=19 to Z=40 without atmosphere

27 control or other concerns typically encountered with XRF systems. We developed data

28 correction protocols for the portable X-ray fluorescence spectrometer on the *JOIDES*

29 *Resolution,* and used the instrument to make rapid and precise quantitative abundance

30 measurements on a menu of key elements. The robustness of the pXRF in analyzing rock

31 surfaces and powders permitted us to obtain rapid, high density results on freshly recovered

32 core materials, which made the instrument a highly valued addition to our shipboard

33 analytical capabilities during IODP Expedition 352. With an awareness of the limitations and

constraints of the method, and care in the instrument's calibration, portable X-ray

fluorescence spectrometers can provide important new capabilities for rapid, quantitative

sample characterization at sea, and offer critical information to operational decision making

onboard geoscience research vessels.

Acknowledgements

.

References

Canadian Certified Reference Materials Project, 1995, Certificate of Analysis, Provisional Values, Till-1, Till-2, Till-3, and Till-4, Geochemical Soil and Till Reference Materials.

Christie DM, Pedersen RB, Miller DJ, Shipboard Scientific Party, 2001, Mantle reservoirs and migration associated with Australian-Antarctic rifting. Proceedings of the ODP, initial reports 187. http://www-odp.tamu.edu/publications/187_IR/ 187ir.htm

Conrey, R.M., Goodman-Elgar, M., Bettencourt, N., Seyfarth, A., Van Hoose, A., and Wolff, J.A., 2014, Calibration of a portable X-ray fluorescence spectrometer in the analysis of archaeological samples using influence coefficients. *Geochemistry: Exploration, Environment, Analysis*, Geol. Soc. London, http://dx.doi.org/10.1144/geochem2013-198

Drake, L., 2014, XRF User guide: Concepts, http://www.xrf.guru/styled-12/page67/index.html

Gillis, K.M., Snow, J.E., Klaus, A., and the Expedition 345 Scientists, 2014, *Proceedings of the Integrated Ocean Drilling Program, 345*: College Station, TX (International Ocean Discovery Program). http://dx.doi.org/10.2204/iodp.proc.345.2014

Godard, M., Ryan, J.G., Shervais, J., Whattam, S., Sakuyama, T., Kirchenbaur, M., Li, H., Nelson, W., Prytulak, J., Pearce, J., Reagan, M, and the Expedition 352 Scientific Team, 2015, Geochemistry of Bonin fore-arc volcanic sequence: results from IODP Expedition 352. 2015 AGU Fall Meeting, Abstract T41E-2948.

Hastie, A.R., Kerr, A.C., Pearce, J.A., and Mitchell, S.F., 2007, Classification of altered Volcanic island arc rocks using immobile trace elements: development of the Th–Co discrimination diagram, Jour. Petrol., 48, 2341-2357, 2007.

Hennekam, R., and de Lange, G., 2012, X-ray fluorescence core scanning of wet marine sediments: methods to improve quality and reproducibility of high resolution paleoenvironmental records, Limnol. Oceanogr.: Methods, 10, 991–1003

Hu, W., Huang, B., Weindorf, D.C., and Chen, Y., 2014, Metals analysis of agricultural soils via portable X-ray fluorescence spectrometry. Bull. Environ. Contam. Toxicol., 92, 420–426.

Jan Weltje, G., and Tjallangii, R., 2008, Calibration of XRF core scanners for quantitative geochemical logging of sediment cores: Theory and application. Earth Planet. Sci. Lett., 224, 423-438.

1 Jochum, K.P., Nohl, U., Herwig, K., Lammel, E., Stoll, B., Hofmann A.W., 2005,
2 GeoReM: A new geochemical database for reference materials and isotopic standards.
3 Geostandards and Geoanalytical Research, 29, 333-338.
4 Kido, Y., Koshikawa, T., and Tada, R., 2006, Rapid and quantitative major element
5 analysis method for wet, fine-grained sediments using an XRF microscanner, Marine
6 Geology, 229, 209–225
7 Koppers, A.A.P., Yamazaki, T., Geldmacher, J., and the Expedition 330 Scientists, 2012.
8 *Proceedings of the Integrated Ocean Drilling Program, 330*: Tokyo (Integrated Ocean
9 Drilling Program Management International, Inc.).
10 http://dx.doi.org/10.2204/iodp.proc.330.2012
11 Liang, L., Sun, Y., Yao, Z., Liu, Y., and Wu, F., 2012, Evaluation of high-resolution
12 elemental analyses of Chinese loess deposits measured by X-ray fluorescence core scanner,
13 Catena, 92, 75-82.
14 Lowemark, L., Chen, H.-F., Yang, T.-N., Kylander, M., Y.-W. Hsu, T.-Q. Lee, Song, S.-
15 R., and Jarvis, S., 2011, Normalizing XRF-scanner data: A cautionary note on the
16 interpretation of high-resolution records from organic-rich lakes, Journal of Asian Earth
17 Sciences, 40, 1250-1256.
18 Potts, P.J., 1992, *A Handbook of Silicate Rock Analysis*. New York, Springer Science
19 Business Media, 630 p.
20 Potts, P.J., and West, M. (eds.), 2008, *Portable X-ray Fluorescence Spectrometry:*
21 *Capabilities for In Situ Analysis.* Royal Society of Chemistry, http://pubs.rsc.org |
22 doi:10.1039/9781847558640-00001
23 Reagan, M.K., Ishizuka, O., Stern, R.J., Kelley, K.A., Ohara, Y., Blichert-Toft, J.,
24 Bloomer, S.H.., Cash, J., Fryer, P., Hanan, B.B., Hickey-Vargas, R., Ishii, T., Kimura, J-I.,
25 Peate, D.W., Rowe, M.C., and Woods, M., 2010, Fore-arc basalts and subduction initiation in
26 the Izu-Bonin-Mariana system. Geochemistry Geophysics Geosystems, 11, Q03X12,
27 doi:10.1029/2009GC002871
28 Reagan, M.K., Pearce, J.A., Petronotis, K.E., and the Expedition 352 Scientists, 2015,
29 *Proceedings of the International Ocean Discovery Program: Volume 352: Izu-Bonin-*
30 *Mariana Fore Arc*. doi:/10.14379/iodp.proc.352.2015.
31 Reynolds, R.C. Jr., 1963, Matrix corrections in trace element analysis by X-ray
32 fluorescence: estimation of mass absorption coefficient by Compton scattering. American
33 Mineralogist, 48, 1133-1143.

Rowe, H., Hughes N., and Robinson, K., The quantification and application of handheld energy-dispersive x-ray fluorescence (ED-XRF) in mudrock chemostratigraphy and geochemistry, Chem. Geol., 324-325, 122-131.

Shervais, J., Haugen, E., Ryan, J.G., Godard, M., Prytulak, J., Shimizu, K., Chapman, T., Nelson, W., Heaton, D., Li, H., Kirchenbaur, M., Li, Y., Whattam, S., Reagan, M., and Pearce, J. (2016) Chemostratigraphy of subduction initiation: IODP Expedition 352 boninite and FAB. Geological Society of America Abstracts with Programs, 48:7, doi: 10.1130/abs/2016AM-283837

Swanhart, S., Weindorf, D.C., Chakraborty, S., Bakr, N., Zhu, Y., Nelson, C., Shook, K., and Acree, A., 2014, Soil salinity measurement via portable X-ray fluorescence spectrometry. Soil Sci., 179, 417–423.

Teagle, D.A.H., Ildefonse, B., Blum, P., and the Expedition 335 Scientists, 2012, *Proceedings of the Integrated Ocean Drilling Program, 335*, Tokyo (Integrated Ocean Drilling Program Management International, Inc.), http://dx.doi.org/10.2204/iodp.proc.335.2012

Thermo Scientific, 2010, *Thermo Fisher Scientific Niton Analyzers: XL3 Users Guide, Version 7.0, Revision A.*

Thermo Scientific, 2016, Thermo Scientific Niton XL3t GOLDD+ Portable XRF Analyzer. [http://pdf.directindustry.com/pdf/thermo-fisher-scientific/thermo-scientific-niton-xl3t-goldd-spec-sheet/25842-152207.html]

Tykot, R.H., Using nondestructive portable X-ray fluorescence spectrometers on stone, ceramics, metals, and other materials in museums: advantages and limitations, Appl. Spectroscopy, 70, 42-56, 2016.

US Environmental Protection Agency, 2007, Method 6200. Field portable X-ray fluorescence spectrometry for the determination of elemental concentrations in soil and sediment. http://www.epa.gov/sites/production/files/2015-12/documents/6200.pdf .

Weindorf, D.C., Zhu, Y., McDaniel P., Valerio, M., Lynn, L., Michaelson, G., Clark M, and Ping, C.L., 2012, Characterizing soils via portable x-ray fluorescence spectrometer: 2. spodic and albic horizons. Geoderma, 189-190, 268-277.

Wien, K., Wissman, D., Kolling, M. and Schulz, H.D., 2005, Fast application of X-ray fluorescence spectrometry aboard ship: how good is the new portable Spectro Xepos analyser? Geo-Marine Letters, 25, 248-264.

Zhu, Y., Weindorf, D.C., and Zhang, W., 2011, Characterizing soils using a portable X-

1   ray fluorescence spectrometer: 1. Soil texture. Geoderma, 167-168, 167-177.
2
3
4

1 Figures:
2
3 Figure 1. Photographs of the shipboard Fisher-Niton GOLDDxlt pXRF instrument and its
4 two different sample mounts, after Reagan et al (2015). a) The pXRF mounted in its "Field
5 Mate" sample holder. b) The IODP-made holder for longer core samples. The pXRF mounts
6 from below. Samples are placed on rectangular aperture visible in the shielded sample
7 chamber.
8
9 Figure 2: Working curves constructed for the elements analysed by pXRF, essentially plots of
10 pXRF measured concentrations vs. accepted values for the reference materials examined.
11 Standard reference materials used included BHVO-2, BCR-2, JB-2, JB-3, AGV-1, MRG-1,
12 JP-1, and DTS-1; consensus values from GeoREM (Jochum et al 2005). Also included were
13 boninite samples CHI 40618, CHI 32108, and CHI 88X (Pearce, unpublished data), to extend
14 our concentration ranges into those likely to be encountered in Expedition 352 boninite
15 samples. a) K_2O. b) TiO_2. c) CaO. d) Sr. e) Rb. f) Cr. g) Fe_2O_3. h) Zn. i) V. j) MnO. k)Cu.
16
17 Figure 3: Plots of a)TiO_2, b)CaO, c)K_2O, d)Sr, e)Cr, and f)Zr for U1440B sample powders
18 and associated thin section residues. Uncertainties are as reported by the pXRF. Solid lines
19 and the associated equations are linear regression correlations for the data, and dotted lines
20 reflect 95% confidence intervals. The elements least affected by secondary alteration
21 processes show the most uniformity between powdered and solid samples.
22
23 Figure 4: Plots of a) a)TiO_2, b)CaO, c)K2O, d)Cr, e)Sr, and f)Zr for Hole U1440B samples
24 comparing pXRF (red circles), and wavelength dispersive XRF (blue triangles) to shipboard
25 ICP-OES results on Expedition 352 "POOL" sample powders. Wavelength dispersive XRF
26 results are from Shervais et al (2016) and Godard et al (2015). Regression lines, equations,
27 and 95% confidence intervals as in Figure 3.
28
29 Figure 5: Chemostratigraphic correlation plots after Reagan et al (2015) from IODP
30 Expedition 352 Site U1440B, highlighting the use of TiO_2 and Cr concentrations to identify
31 different magmatic units, despite very poor sample recovery (~12%).
32
33 Figure 6: Correlations between Ti/Zr, Cr, and magnetic susceptibility for IODP Expedition
34 352 Holes U1439C and U1442A, from Reagan et al (2015), along with a comparative outline

1   of the occurrences of high-silica and low-silica boninites in each section, as well as positions

2   of observed zones of melt mixing. The linked geochemical and physical property

3   relationships were used both to define magmatic units downhole, and to document the marked

4   stratigraphic differences between the two nearby (<1 km apart) sites.

5

6

7

8   Tables:

9

10   Table 1: List of elements measured via pXRF during IODP Expedition 352, analytical

11   conditions and detection limits.

12

13   Table 2: Standard Reference Materials used in pXRF onshore calibration and to construct

14   pXRF data correction curves. Standard data based on consensus values from GeoReM

15   (Jochum et al 2005); boninite data from J. Pearce.

16

17   Table 3: Long-term reproducibility of the shipboard Fisher Niton GOLDD+XL3t portable

18   XRF instrument.

19

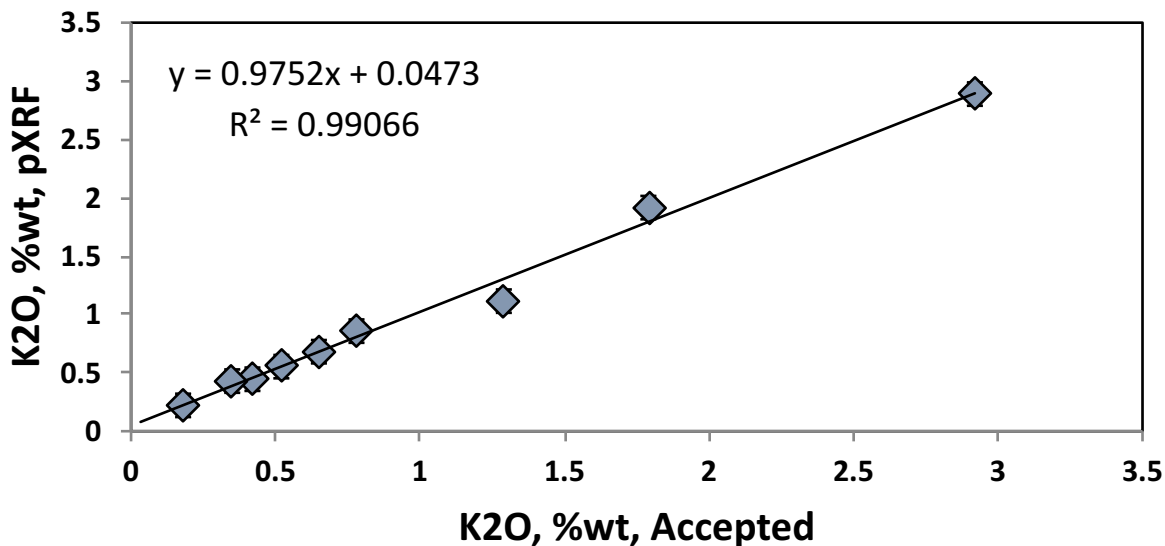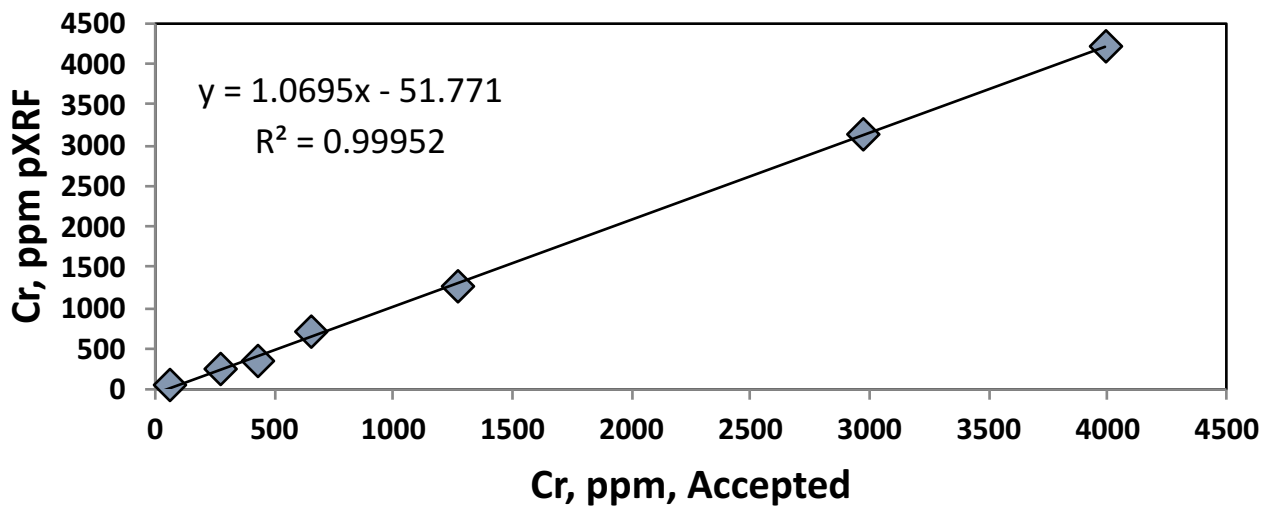20   Table 4: pXRF reproducibility and accuracy on rock surfaces.

Fig 1

a.

b.

Fig 2 a, b, c

Fig 2 d,e,f

$y = 0.9498x + 3.7583$
$R^2 = 0.99841$

$y = 0.9201x - 0.7302$
$R^2 = 0.99536$

$y = 1.0695x - 51.771$
$R^2 = 0.99952$

Fig 2 g,h,i

$y = 1.2077x - 2.454$
$R^2 = 0.96235$

$y = 0.9516x - 1.4275$
$R^2 = 0.97908$

$y = 0.9516x + 32.424$
$R^2 = 0.84475$
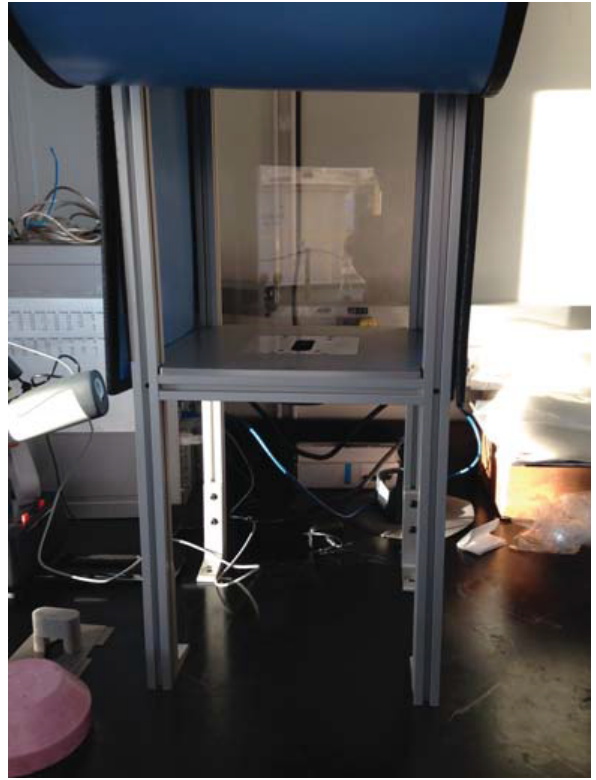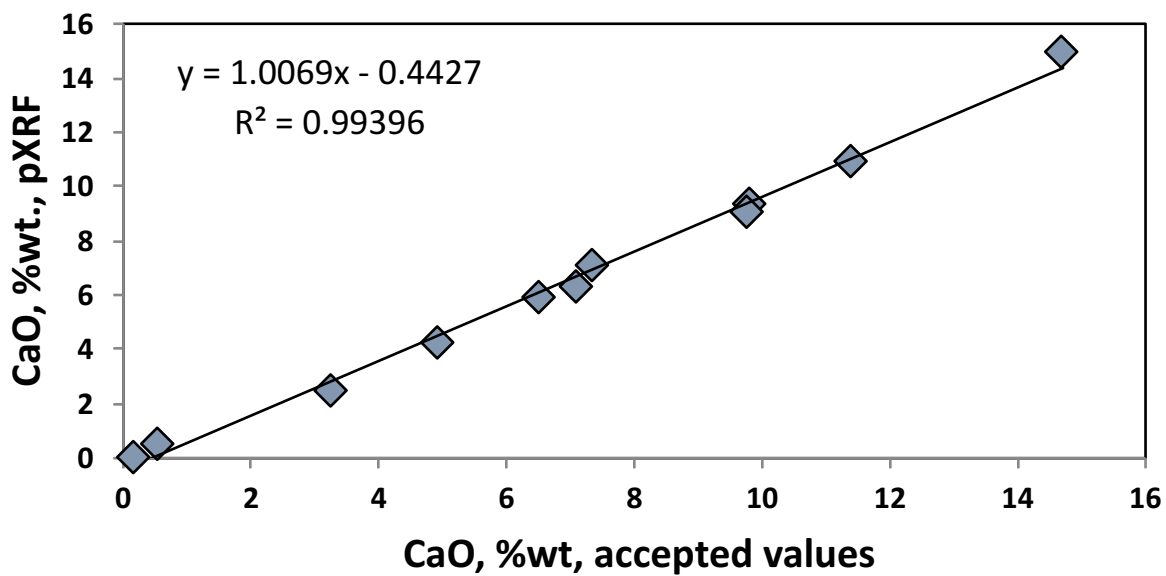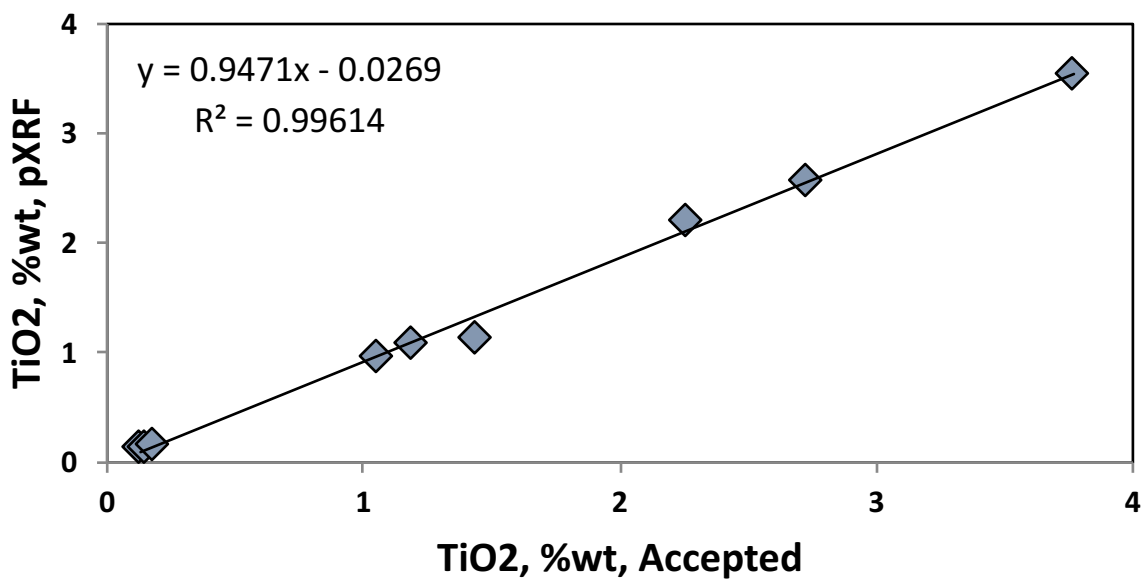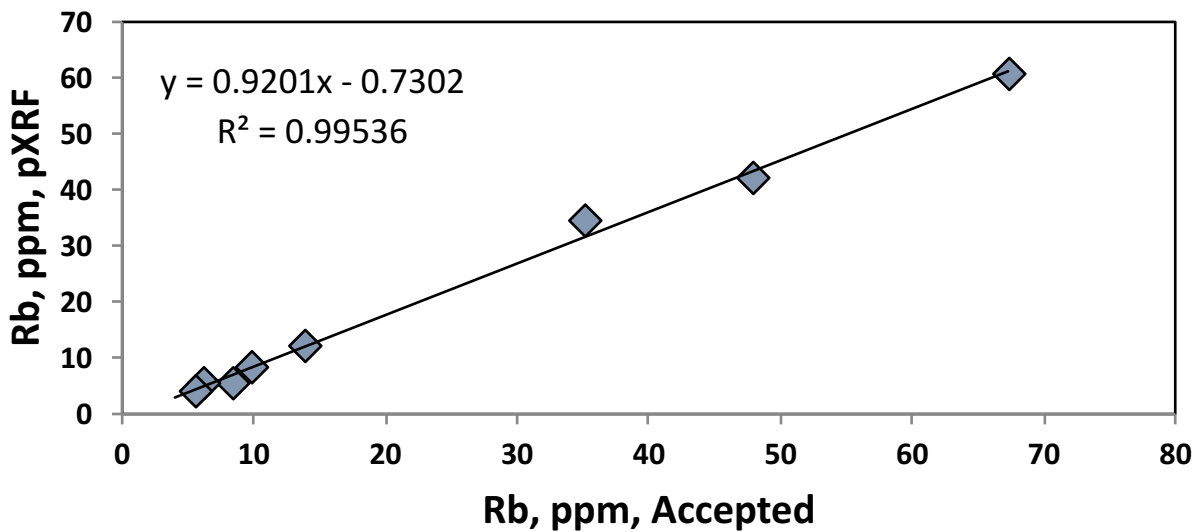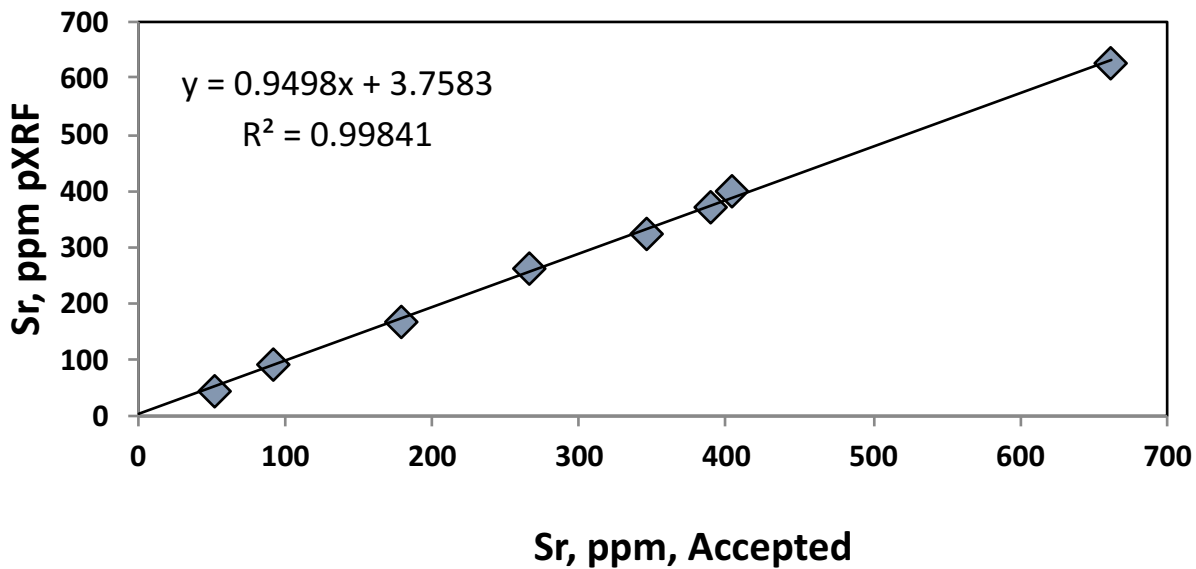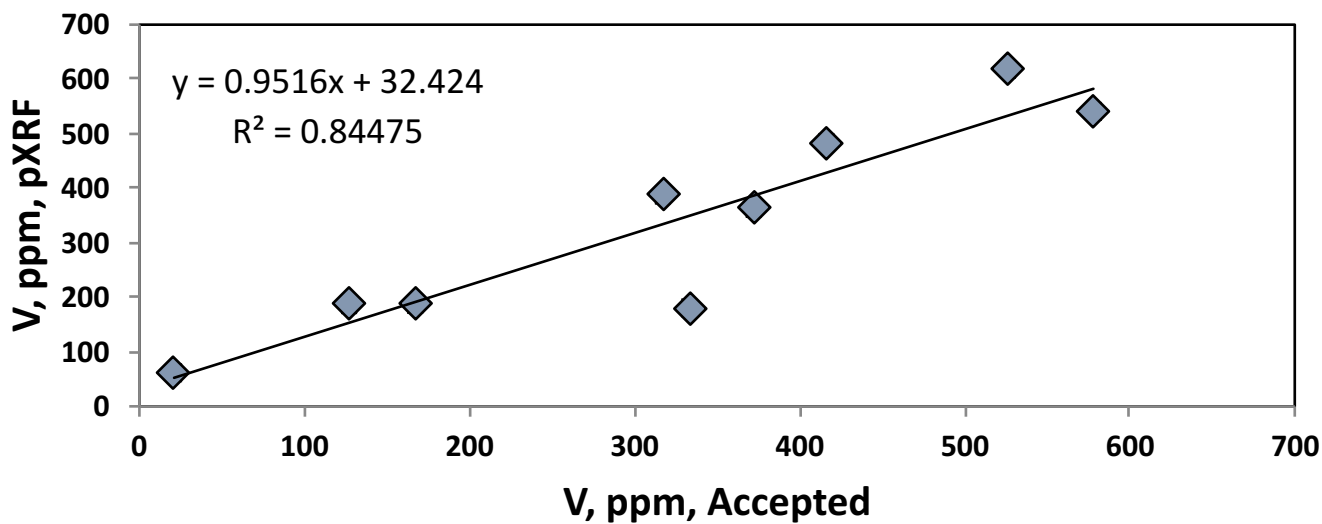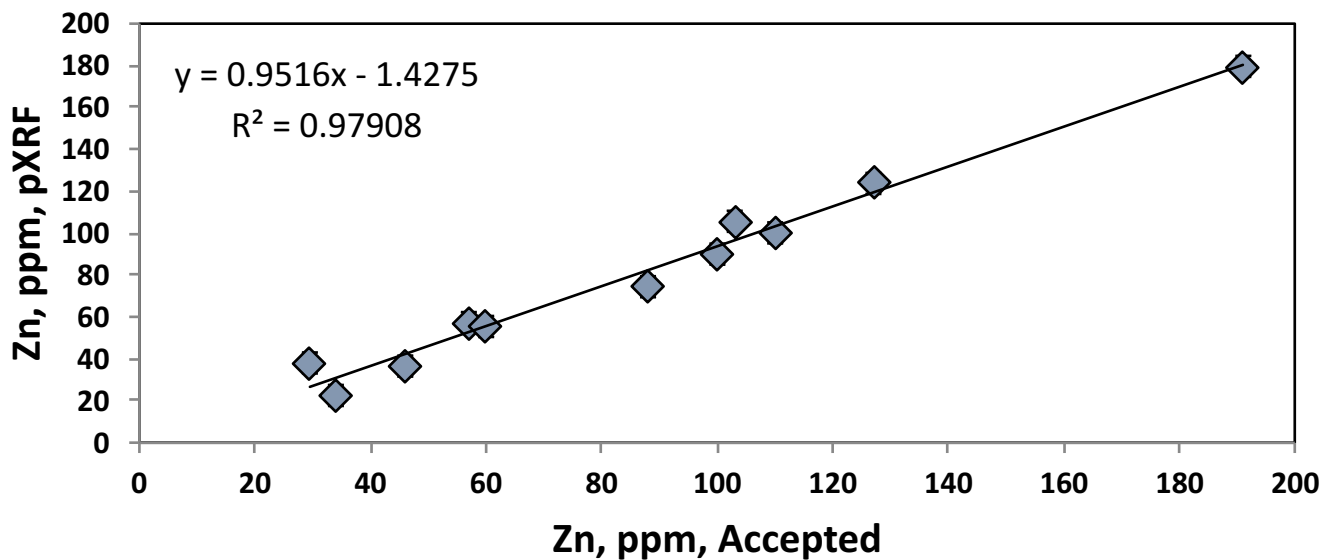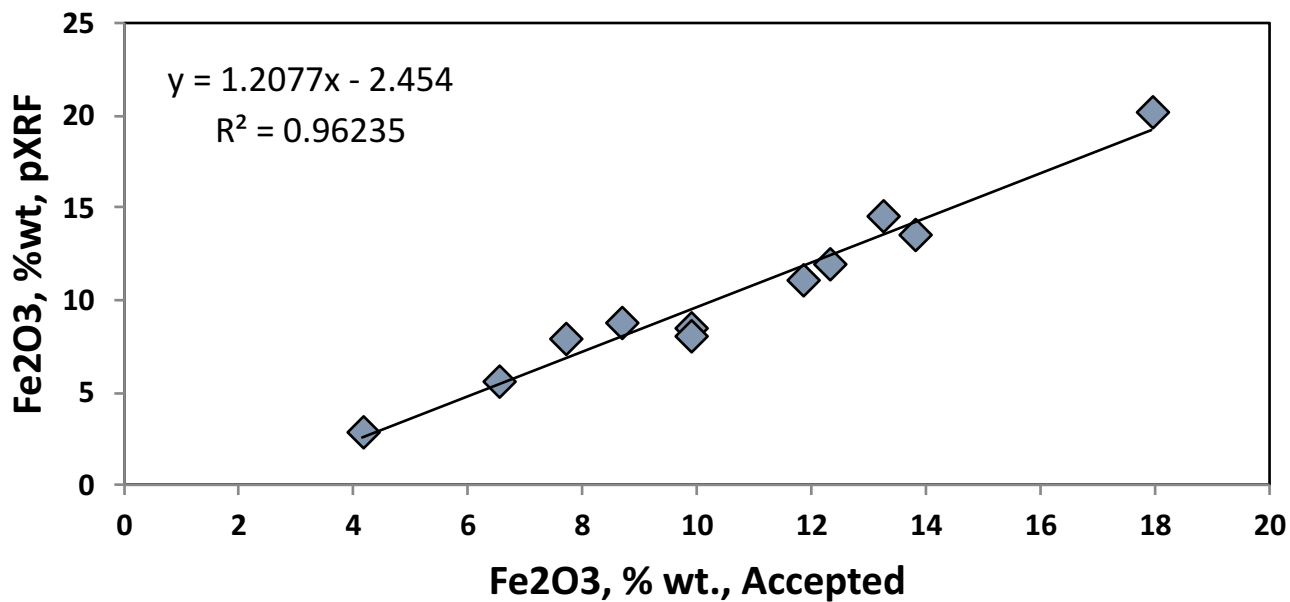
Figure 2 j,k

Figure 3

Figure 4

a.

TiO2 XRF f=0.997959**X**+0.0260505
r = 0.997942

TiO2 pXRF
f=0.966119**X**+0.0476052
r = 0.940105

TiO2 ICP-OES

b.

CaO XRF f=1.01585**X**−0.128632
r = 0.994909

CaO pXRF
f=0.949472**X**−0.318074
r = 0.94913

CaO ICP-OES

c.

K2O XRF   f=0.940951**X**−0.0167842
r = 0.997274

K2O pXRF
f=0.969561**X**+0.0229016
r = 0.987674

K2O ICP-OES

d.

Cr XRF   f=0.896345**X**+33.7046
r = 0.997094

Cr pXRF
f=0.723303**X**+18.9573
r = 0.987172

Cr ICP-OES

e.

Sr XRF

f=1.07495**X**−8.66444
r = 0.990215

Sr pXRF

f=0.962283**X**+3.00988
r = 0.981725

Sr ICP-OES

f.

Zr XRF

f=1.14124**X**−3.1455
r = 0.963501

Zr pXRF

f=0.725936**X**+6.00767
r = 0.926066

Zr ICP-OES

Figure 5

Figure 6

Hole U1439C

Hole U1442A

Revised tables in pdf format
Click here to download Table: Revised pXRF paper tables.pdf

Table 1: Reference materials used in pXRF on-shore calibration, and to construct pXRF correction curves
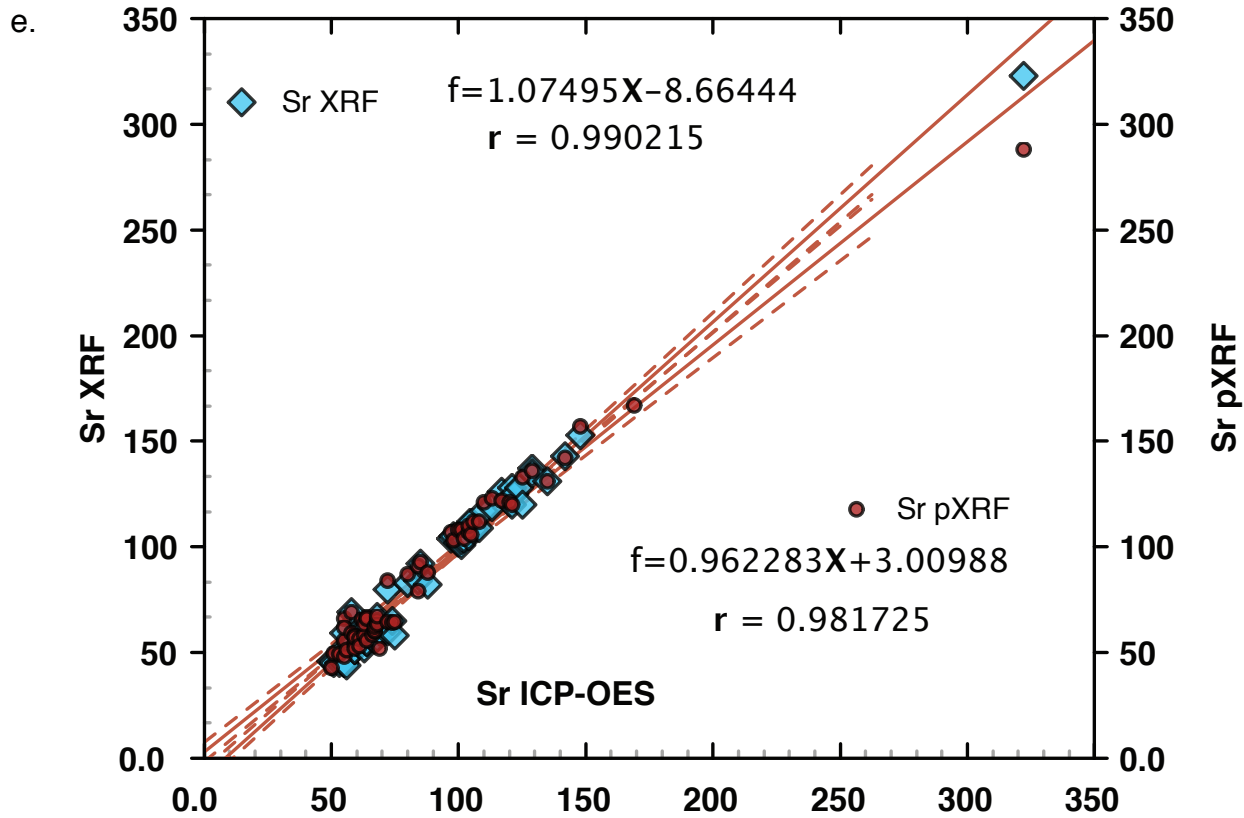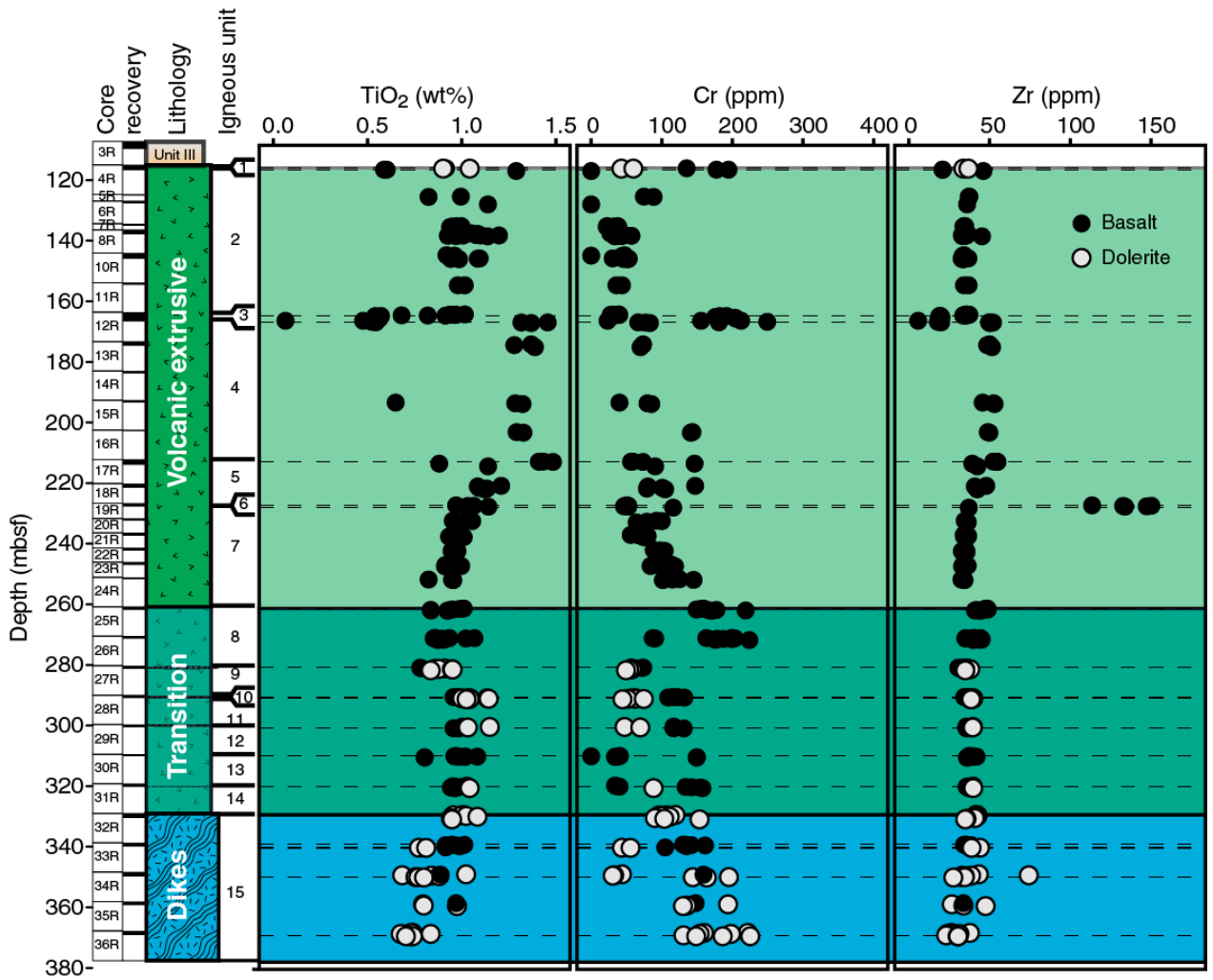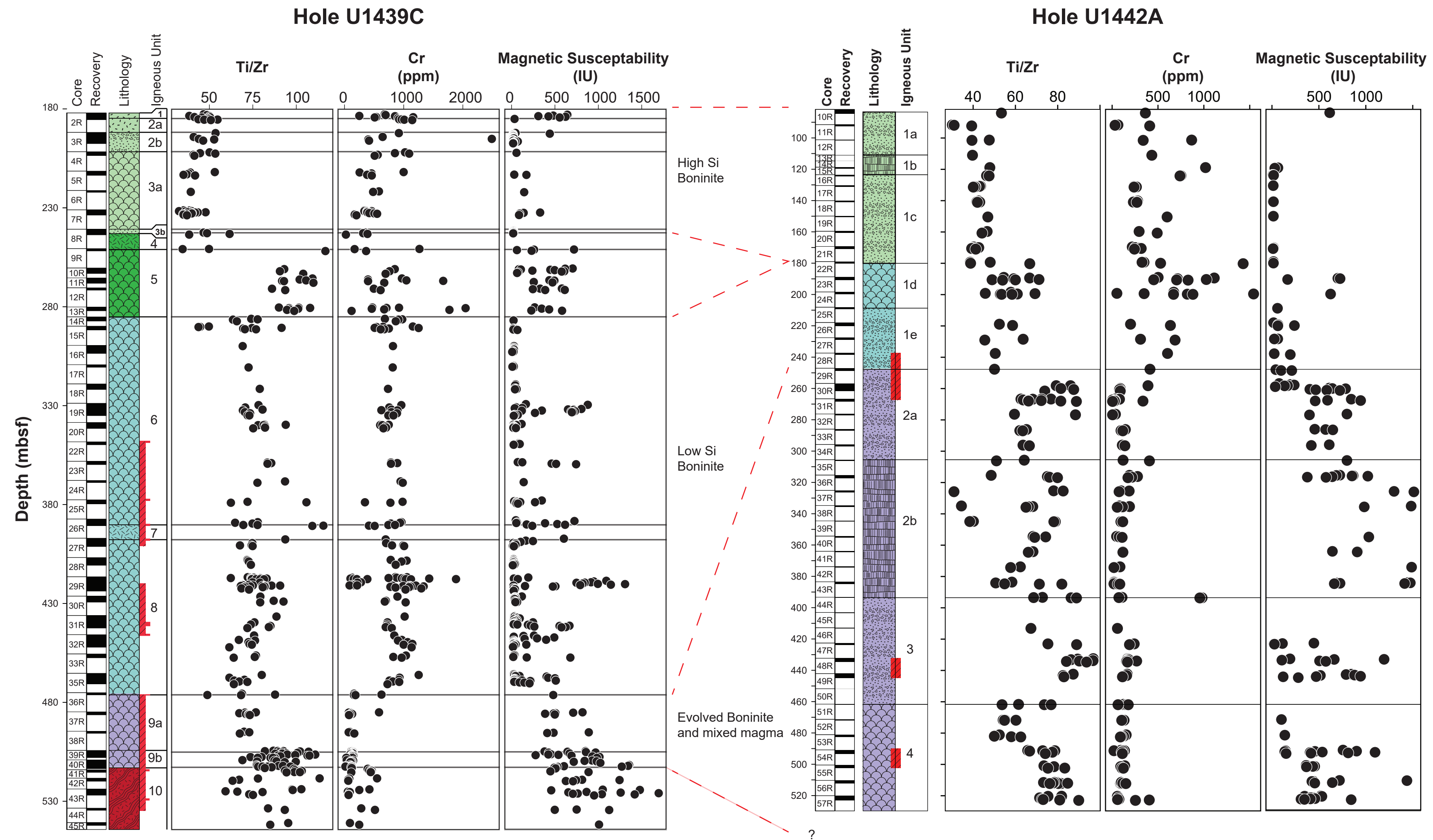
	TiO2 (wt%)	Fe2O3 (wt%)	CaO (wt%)	K2O (wt%)	Zr (ppm)	Sr (ppm)	Rb (ppm)	Zn (ppm)	Cu (ppm)	MnO (wt%)	Cr (ppm)	V (ppm)
Shore-based calibration (Compton Normalization)												
CCRMP TILL-4	0.81	5.63	1.25	3.25	385	109	161	70	237	0.06	53	67
Shipboard calibration:												
BHVO-2	2.73	12.25	11.4	0.52	172	396	9.11	103	127	0.168	280	317
BCR-2	2.36	13.8	7.12	1.79	188	346	48	127	19	0.175	18	416
JB-2	1.19	13.22	9.82	0.42	52	178	6.2	110	227	0.218	27.4	578
JB-3	1.44	11.84	9.79	0.78	97.8	403	15.1	100	194	0.177	58.1	372
AGV-1	1.05	6.52	4.94	2.92	227	662	67.3	88	60	0.098	10.1	333
DTS-1	0.005	8.68	0.17	0.001	4	0.32	0.058	46	7.1	0.121	3990	11
MRG	3.77	17.93	14.71	0.18	108	266	8.5	191	134	0.17	430	526
JP-1	--	7.7	0.56	0.033	6	3.3	4	29.5	5.7	0.12	2970	29
CH40618*	0.13	9.9	6.53	0.35	13.2	51	5.7	57	41	0.14	1275	167
CH32108*	0.15	9.87	7.37	0.65	20.5	239	14	60	70	0.16	660	127
CHX88A*	0.18	4.15	3.28	1.29	54.5	91	35.2	34	63	0.04	10	21

USGS, GSJ and CCRMP reference materials data from Jochum et al (2005)

* Data from J. Pearce, unpublished

Table 2: List of elements measured via pXRF during IODP Expedition 352, analytical conditions and detection limits*

Analyzed elements	Filter Position	Detection Limit * (ppm)
Sr	Main	3
Rb	Main	2
Zn	Main	8
Cu	Main	15
Fe	Main	30
Mn	Main	25
Cr	Main/Light	25
V	Main/Light	15
Ti	Main/Light	30
Ca	Light	40
K	Light	75

* As provided by the manufacturer

Table 3: Long-term reproducibility of the shipboard Fisher Niton GOLDD+ XL3t portable XRF instrument

	TiO2 (wt%)	Fe2O3 (wt%)	CaO (wt%)	K2O (wt%)	Zr (ppm)	Sr (ppm)	Rb (ppm)	Zn (ppm)	Cu (ppm)	Mn (ppm)	Cr (ppm)	V (ppm)
BHVO-2 (n =35; 18 Aug - 22 Sept, 2014)	2.65	9.79	10.74	0.56	167	389	9	105	142	1367	221	397
Standard deviation:	0.03	0.05	0.13	0.01	1	2	0.5	2	4	21	6	13
RSD (%):	1.1	0.5	1.2	1.8	0.8	0.5	5.2	2.3	2.6	1.5	2.8	3.2
Accuracy (%):	-2.9	-25.1*	-6.2	6.7	-3	-1.8	-6.3	1.9	10.8	3.7	-26.7*	20.2*
BHVO-2 preferred values:	2.73	12.25	11.4	0.52	172	396	9.11	103	127	1317	280	317

* See discussion in text re: accuracy of Fe, V, and Cr determinations.

Table 4: pXRF Reproducibility and accuracy on rock surfaces

Sample 1092-20	pXRF	2 σ Standard deviation (n = 10)	Coefficient of variation (%)	Variation from reported values (%)	1092-20 values (Reagan et al., 2010)
Major element oxide (wt%):					
TiO_2	1.03	0.04	4	-0.39	1.03
Fe_2O_{3*}	10.72	0.17	1.59	-10.77	12.02
CaO	11.35	0.31	2.72	-8.21	12.36
K_2O	0.24	0.04	16.95	24.37	0.19
Trace element (ppm):					
Sr	68.33	2.25	3.29	-0.54	68.7
Rb	4.04	0.88	21.66	3.7	3.9
Zn	105.24	5.41	5.14	-	-
Cu	179.71	15.36	8.55	-	-
Cr*	225.09	14.04	6.24	-21.02	285
Zr	54.84	2.12	3.86	-4.29	57.3

* Sources of Fe and Cr variation from accepted values are as discussed in the text.